


 Cite this: *RSC Adv.*, 2025, 15, 21168

Study of diclofenac distribution in aqueous two-phase PEG/salt/water systems†

 Diana Esmeralda Martínez-Rodríguez,^{id}^a Edgar Daniel Martínez-Rodríguez,^{id}^{bc} Liliana Hernández-Perales,^{id}^a María del Pilar González-Muñoz^{id}^a and Mario Avila-Rodríguez^{id}^{*a}

Diclofenac is a nonsteroidal anti-inflammatory drug (NSAID). Due to its extensive use, it has been detected in various environmental compartments, where it has been shown to exert adverse effects on living organisms. This underscores the need to develop efficient and environmentally benign removal strategies. Aqueous Two-Phase Systems (ATPS) offer a promising alternative for liquid–liquid extraction without the use of organic solvents, providing a sustainable separation technique. This study evaluated the effectiveness of diclofenac extraction using ATPS. Results demonstrated that, at low drug concentrations (10 ppm), extraction yields exceeded 95% across all systems tested, regardless of whether the pH values were above or below the pK_a of diclofenac. The ATPS composed of polyethylene glycol (PEG) 1000 g mol⁻¹ at 25.5% w w⁻¹ and sodium citrate at 21.5% w w⁻¹ was identified as the most efficient, achieving an extraction efficiency of up to 99.9% and minimal mass transfer of PEG and salt between phases. UV-Vis spectroscopy analysis suggests that the drug's phase transfer occurs via hydrogen bond formation between diclofenac and PEG. The proposed method exhibits high efficiency for diclofenac recovery and stands out for its low environmental impact.

 Received 13th February 2025
 Accepted 7th June 2025

DOI: 10.1039/d5ra01070e

rsc.li/rsc-advances

1 Introduction

Emerging pollutants are defined as compounds that are not currently regulated by any environmental legislation. Due to the lack of regulation, their potential harmful effects on the environment and living organisms remain largely unknown.¹ Among the pharmaceutical residues most frequently detected in aquatic environments are carbamazepine and diclofenac, with estimated global annual consumption of 1014 and 940 tons, respectively.²

Diclofenac (2-(2,6-dichloroanilino)phenylacetic acid) (DFC) (Fig. 1), is a nonsteroidal anti-inflammatory drug (NSAID) with a water solubility of 2.37 mg L⁻¹ (25 °C) and a dissociation constant (pK_a) of 4.15.³

DFC is used therapeutically as an analgesic, antipyretic, and anti-inflammatory agent⁴ and it has also been shown to possess angiogenic activity.⁵ The drug is available in oral, intramuscular, and topical formulations, most of which are over-the-counter and relatively inexpensive,⁴ contributing to its

widespread use as one of the most commonly used anti-inflammatory drugs worldwide. However, prolonged administration of DFC has been associated with hepatotoxicity, nephrotoxicity, and an increased risk of myocardial infarction.^{4,6} Moreover, DFC metabolites have been shown to exhibit greater toxicity than the parent compound.² Environmental compartments in which these pollutants are most frequently detected include surface water, groundwater, drinking water, seawater, wastewater, soil, sediments, suspended solids, sludge from wastewater treatment plants, and leachates.⁷ These compounds have also been detected in various species, including aquatic animals, mammals, birds, fruits, and plant leaves.⁷ Given their potential adverse health effects⁸ and environmental impact, the development of new methods for detecting and evaluating

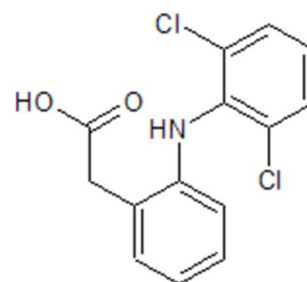


Fig. 1 Chemical structure of diclofenac.

^aDepartamento de Química, División de Ciencias Naturales y Exactas, Universidad de Guanajuato, Cerro de la Venada S/N, Pueblito de Rocha, 36040 Guanajuato, Mexico. E-mail: avilam@ugto.mx

^bSecretaría de Ciencia, Humanidades, Tecnologías e Innovación (SECIHTI), Mexico City, 03940, Mexico

^cCentro de Investigación en Matemáticas, CIMAT, 36023 Guanajuato, Mexico

† Electronic supplementary information (ESI) available. See DOI: <https://doi.org/10.1039/d5ra01070e>



remediation or elimination strategies for DFC and other pollutants is essential.

An efficient and environmentally friendly alternative for drug recovery is the use of Aqueous Two-Phase Systems (ATPS), which retain the advantages of conventional Liquid–Liquid Extraction (LLE) while eliminating the use of organic solvents with high vapor pressure. ATPS operate based on the differential partitioning of solutes within a two-phase system composed predominantly of water (70–90%, depending on the type of system).⁹ These systems are formed by mixing two water-soluble components, which, upon reaching equilibrium, separate into two immiscible aqueous phases.

A wide range of ATPS types is currently available, including polymer/polymer (of different chemical nature), polymer/salt, and systems incorporating ionic liquids, copolymers, or deep eutectic solvents. ATPS are highly versatile and have been successfully employed for the partitioning of metal ions, drugs, nanomaterials, and metabolites, among other compounds.^{10,11} Specifically, this technique has been used for the recovery, separation, and concentration of roxithromycin,¹² sulfonamides,¹³ and tetracycline¹⁴ from water samples, animal-derived food products, and plant matrices. These systems are also being explored for future applications in the manufacturing of biopharmaceuticals¹⁵ and the removal of pharmaceutical contaminants from water samples.¹⁶ Furthermore, due to their concentration effect, ATPS can enhance the detection and recovery of drug residues in water bodies, even at trace levels (*i.e.*, emerging pollutants).

Various applications of ATPS have been explored in the pharmaceutical industry, owing to their high capacity to efficiently and selectively separate, purify, and concentrate solutes in a mild environment, facilitated by the use of low-toxicity compounds and their predominantly aqueous composition. Table 1 presents several examples of these applications. These systems represent a key tool in drug development, pharmaceutical biotechnology, and biological therapies. Although this review is not exhaustive, it provides a clear overview of the potential applications of ATPS in this field.

Despite the promising laboratory results, the industrial application of ATPS faces technical, economic, and operational limitations. Key challenges include process scalability, high material costs, and the need for additional downstream treatments to recover the target compound. The use of copolymers or ionic liquids, while sometimes effective, may compromise the sustainability of the process due to their toxicity and cost.

From a process engineering perspective, optimizing phase stability, separation kinetics, and partitioning efficiency is essential. Process design, variable control, and compliance with stringent regulations—particularly in the pharmaceutical and food industries—must also be carefully addressed.

Nevertheless, the advantages of ATPS—such as low energy consumption, biocompatibility, high selectivity, and phase reusability—support their development as a green technology. Successful scale-up examples and potential long-term cost savings further strengthen their promise for sustainable pharmaceutical and environmental applications.

In the existing literature on DFC extraction using ATPS, only two studies have explored this application, and none have investigated the specific system evaluated in the present study. Ahsaie *et al.*²² reported the use of ATPS composed of various copolymers and dextran, achieving extraction efficiencies between 39% and 99.6%, depending on the system composition and operational conditions. The authors attributed the preferential partitioning of DFC into the top phase to its hydrophobic nature and the higher hydrophobicity of the copolymer-rich phase. Priyanka *et al.*²³ employed ATPS based on ionic liquids—both mono- and dicationic species derived from imidazolium, pyrrolidinium, morpholinium, and ammonium (with bromide as the common anion) combined with potassium salts. Reported extraction efficiencies ranged from 80% to 100%, depending on the ATPS conformation. The authors concluded that systems maintaining either acidic or alkaline conditions achieved high extraction efficiencies regardless of pH, suggesting that electrostatic interactions between the ionic liquid species and the charged form of DFC play a negligible role. They further highlighted the suitability of highly hydrophobic ionic

Table 1 Applications, advantages, and examples of ATPS in the pharmaceutical industry

Application	Advantage	Examples	Reference
Purification of proteins and enzymes	Efficient separation High recovery Preservation of biological activity	Purification of therapeutic proteins such as insulin, interferons, or monoclonal antibodies	17
Extraction of antibiotics and metabolites	Improved recovery of natural products from fermentation broths	Penicillin separation	18
Separation and isolation of cells	Gentle process that maintains cell viability	Separation of stem cells, immunological cells, and bacteria	19
Design of controlled extraction systems, microencapsulation, and product stability	ATPS can be designed for drug encapsulation or controlled release. Microencapsulation of pharmaceutical compounds improves stability and shelf life	Hydrogels and polymersomes Formulation of micro/nanoparticles	20
Extraction and purification of DNA and RNA	Useful for isolating genetic material in diagnostic or gene therapy processes	Plasmid DNA	21



Table 2 Summary of chemical compounds^a

Name of the compound	Molecular formula	Molecular weight (g mol ⁻¹)	CAS number	% purity, grade, other specifications	Source
Polyethylene glycol 400 (PEG-400)	HO-(CH ₂ -CH ₂ -O) _n -H	400	25322-68-3	≥99% reactive grade	Poliolés S.A. de C.V.
Polyethylene glycol 1000 (PEG-1000)	HO-(CH ₂ -CH ₂ -O) _n -H	1000	25322-68-3	≥99% reactive grade	Karal
Sodium citrate dihydrate (Na ₃ Cit)	C ₆ H ₅ Na ₃ O ₇ ·2H ₂ O	294.10	6132-04-3	≥99% reactive grade	Karal
Sodium sulfate anhydrous	Na ₂ SO ₄	142.04	7757-82-6	≥99% reactive grade	Karal
Deionized water	H ₂ O	18.02	7732-18-5	Conductivity 1.5 μmhos cm ⁻¹	Karal
Sodium diclofenac (DFC)	C ₁₄ H ₁₀ Cl ₂ NNaO ₂	318.13	15307-79-6	≥98% reactive grade	Sigma-Aldrich
Buffer pH 4 (sodium citrate)	n.a	n.a	6132-04-3	pH at 25 °C: 3.98–4.02 reactive grade	Karal
Buffer pH 7 (phosphate)	n.a	n.a	7732-18-5	pH at 25 °C: 6.98–7.02 reactive grade	Karal
Buffer pH 10 (sodium borate)	n.a	n.a	7778-77-0		
			7558-79-4		
			7732-18-5		
			1303-96-4		
			7732-18-5		
				pH at 25 °C: 9.98–10.02 reactive grade	Karal

^a n.a. – not applicable.

liquids for the extraction of hydrophobic pharmaceuticals such as sodium diclofenac.

In contrast, the present study utilizes polyethylene glycol/citrate/water and polyethylene glycol/sulfate/water systems, which consist of more accessible and biodegradable components. The selection of these materials enhances the environmental compatibility of the process, supporting ongoing efforts to develop greener and more sustainable extraction methodologies.

This project aims to evaluate the extraction efficiency of sodium diclofenac using ATPS composed of polyethylene glycol (PEG) of different molecular weights (400 g mol⁻¹ and 1000 g mol⁻¹) and two types of sodium salts, one inorganic (sodium sulfate) and one organic (sodium citrate), which has the advantage of being biodegradable, as a sustainable strategy for its recovery from aqueous solutions. To achieve this, various ATPS are formulated by combining PEGs of different molecular weights with salts at varying concentrations (operating points), assessing their influence on phase formation, drug partitioning, diclofenac concentration, and system pH. The extraction efficiency under each condition is determined to identify those that optimize recovery while minimizing environmental impact. Additionally, an extraction mechanism is proposed based on UV/Vis spectroscopy, and the potential of these systems is evaluated as a green alternative for wastewater treatment and their prospective application in the pharmaceutical industry. The working hypothesis posits that PEG/salt/water ATPS promote the partitioning of DFC into the polymer phase, thereby facilitating its recovery and contributing to the development of sustainable remediation technologies.

2 Material and methods

2.1. Materials

Polyethylene glycol (PEG) with molecular weights of 400 g mol⁻¹ and 1000 g mol⁻¹, along with sodium citrate dihydrate and anhydrous sodium sulfate, were used as phase-forming components for the preparation of ATPS. Sodium diclofenac (DFC) was selected as the model compound for the extraction process. All solutions were prepared using deionized water. Detailed information on the materials used, including supplier, CAS number, and purity, is provided in Table 2.

2.2. Methods

2.2.1. Construction of binodal curves. The binodal curves were determined using the cloud-point titration method¹¹ at 298.15 K. A known amount of stock solution of component X (see Table 3) was added to a 25 mL Erlenmeyer flask equipped with a magnetic stirrer and weighed using an analytical balance (OHAUS; Model: Explorer E1240). While stirring, the stock solution of component Y (see Table 3) was added dropwise until the first appearance of turbidity, corresponding to the cloud point. This marked the first data point of the binodal curve. Subsequently, a known amount of diluent (deionized water) was added until the system became clear, indicating that it was below the cloud point. This procedure was repeated



Table 3 Concentrations (% w w⁻¹) of stock solutions used for the construction of each binodal curve of the ATPS at 298.15 K

ATPS	Component X (% w w ⁻¹)	Component Y (% w w ⁻¹)
PEG-400/Sodium citrate	40	50
PEG-400/Sodium sulfate	20	50
PEG-1000/Sodium citrate	40	30
PEG-1000/Sodium sulfate	20	30

systematically until no further turbidity was observed, thereby completing the binodal curve construction.¹¹

2.2.2. Binodal curve modeling. The experimentally determined binodal curves do not capture all possible conditions under which phase separation may occur. Therefore, the development of theoretical binodal curves is useful for complementing the experimental data. These theoretical curves were fitted to the experimental data using the nonlinear empirical equation proposed by Merchuk (eqn (1)).^{24,25}

$$wt^{PEG} = A \exp[(Bwt^{salt^{0.5}}) - (Cwt^{salt^3})] \quad (1)$$

where wt^{PEG} and wt^{salt} represent the concentrations, in percentage by weight, of the polymer and the salt, respectively. Subsequently, the Excel (Microsoft) Solver macro was used to fit the calculated (wt_{cal}^{PEG}) and experimental (wt_{exp}^{PEG}) values by minimizing the objective function U (eqn (2)).

$$U = \sum_{i=1}^N (wt_{cal}^{PEG} - wt_{exp}^{PEG})^2 \quad (2)$$

where wt_{cal}^{PEG} and wt_{exp}^{PEG} represent the calculated and experimental concentrations, in percentage by weight, of the polymer, respectively. N denotes the number of data points on the binodal curve. The standard deviation (sd) was calculated using eqn (3).²⁵

$$sd = \sum_{i=1}^N \left(\frac{(wt_{cal}^{PEG} - wt_{exp}^{PEG})^2}{N} \right)^{0.5} \quad (3)$$

2.2.3. Preparation of ATPS for DFC extraction. Two operating points within the biphasic region were selected for each ATPS evaluated. One point, located near the binodal curve, was

designated as the First Operating Point (FOP), while the other, situated farther from the curve, was referred to as the Last Operating Point (LOP). In all cases, the volume ratio (V_{PP}/V_{SP}) between the polymer phase (PP) and the saline phase (SP) was maintained at 1. Volumes were measured using a graduated cylinder (Pyrex; Model: 2982). Once the total concentrations were established, the procedure outlined in Fig. 2 was followed for drug extraction at 298.15 K. According to the selected system, the appropriate amounts of salt, polymer, and deionized water containing DFC were added to a vial. The mixture was stirred for 10 minutes to ensure complete dissolution of all components. After stirring, the system was allowed to stand for 24 hours to ensure complete phase separation. Subsequently, the drug concentrations in the PP were quantified using UV-Vis spectroscopy.

2.2.4. Theoretical determination of tie-lines. Theoretical tie-lines were used to determine the equilibrium concentrations of polymer and salt in the top and bottom phases. These tie-lines were established using the gravimetric method described by Merchuk.²² Ternary mixtures were prepared at each operating point of the respective ATPS. The samples were stirred for 10 minutes and then left to stand for 24 hours to allow complete phase separation. Subsequently, the phases were carefully separated and weighed. The percentage by weight of polymer (wt^{PEG}) and salt (wt^{salt}) at the top (Top) and bottom (Bot) corresponding phases were calculated using eqn (4)–(7). In these equations, α represents the mass ratio between the saline phase (bottom) and polymer phase (top) phases, and F corresponds to the total concentration of salt and polymer used in the system.

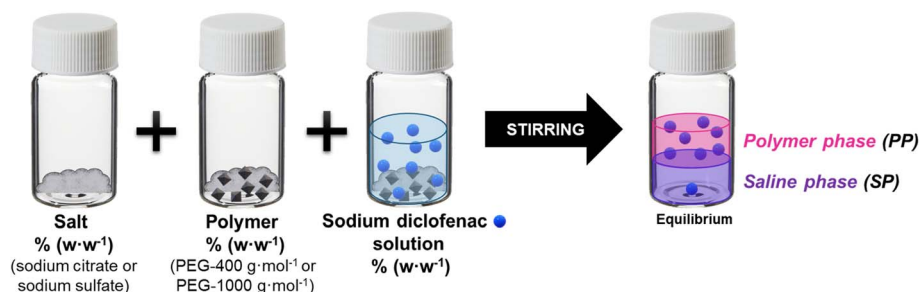
$$(wt^{PEG})_{Top} = A \exp[(B(wt^{salt})_{Top}^{0.5}) - ((wt^{salt})_{Top}^3)] \quad (4)$$

$$(wt^{PEG})_{Bot} = A \exp[(B(wt^{salt})_{Bot}^{0.5}) - ((wt^{salt})_{Bot}^3)] \quad (5)$$

$$(wt^{PEG})_{Top} = \frac{(wt^{PEG})_F}{\alpha} - \frac{1-\alpha}{\alpha} (wt^{PEG})_{Bot} \quad (6)$$

$$(wt^{salt})_{Top} = \frac{(wt^{salt})_F}{\alpha} - \frac{1-\alpha}{\alpha} (wt^{salt})_{Bot} \quad (7)$$

2.2.5. Characterization and quantification of DFC in both phases. The concentration of DFC was determined using ultraviolet-visible (UV-Vis) spectroscopy. Initially, the absorption spectrum of DFC in aqueous solution was obtained to

**Fig. 2** Schematic diagram of the sodium diclofenac extraction process for each ATPS.

enable quantification. A 10 mm quartz cell (PerkinElmer) was used to analyze a 10 ppm DFC solution in deionized water with a UV-Vis spectrophotometer (Varian; Model: Cary 5 Probe) across a wavelength range of 200–400 nm. The maximum absorption wavelength in the aqueous phase was identified at 276 nm.

A calibration curve was constructed using seven DFC solutions of increasing concentrations, prepared in deionized water (without salt). Deionized water served as the blank. Absorbance at 276 nm was measured for each solution using a 10 mm quartz cell. Based on this calibration curve, which showed a correlation coefficient of $R^2 = 0.998$, the initial concentrations of DFC were determined for subsequent extraction experiments.

Following extraction, UV-Vis spectroscopy was employed to quantify DFC in the polymer phase. The absorption spectrum was recorded over the 200–400 nm range using a 10 mm quartz cell. As reference, a blank solution was prepared containing the same concentrations of PEG, salt, and water as the polymer phase, depending on the ATPS composition. The maximum absorption wavelength varied between 280 and 284 nm, depending on the system.

A calibration curve was established using seven drug solutions of increasing concentration, each prepared in the corresponding PEG/salt/water matrix to match the polymer phase conditions. The appropriate blank (polymer phase matrix) was used for each ATPS. Absorbance measurements were taken at the system-specific maximum wavelength, and the extracted DFC concentrations in the polymer phase were calculated accordingly.

The extraction efficiency was determined using eqn (8).

$$\% \text{ extraction} = \frac{\text{mass DFC}_{\text{PP}}}{\text{mass DFC}_0} \times 100 \quad (8)$$

where mass DFC_0 represents the initial mass of DFC, and $\text{mass DFC}_{\text{PP}}$ corresponds to the mass extracted into the polymer phase.

Additionally, the absorption spectra of DFC in deionized water (prior to extraction), as well as those of the PP and SP after the extraction process, were recorded. These spectra were compared with the corresponding blanks (polymer and saline phases solutions containing the same PEG/salt/water concentrations as the selected ATPS). The resulting spectra were subsequently analyzed to evaluate the behavior of DFC in the polymer phase following extraction.

2.2.6. Determination of pH in ATPS without DFC and after the extraction process. The pH of both phases (PP and SP) was measured in the absence of DFC as well as after the extraction process. Measurements were performed using a potentiometer (Metrohm; Model: 913 pH Meter) at 298.15 K. All measurements were performed in triplicate. The potentiometer was calibrated daily using three standardized buffer solutions at 25 °C, traceable to NIST standards (pH 4: potassium biphthalate, pH 7: sodium phosphate, pH 10: sodium borate; all obtained from Karal), ensuring a calibration slope greater than 0.95 in each case.

3 Results and discussion

3.1. Experimental binodal curves, their modeling, and selection of operating points

It is generally recommended that binodal curves be constructed experimentally, as the conditions under which phase separation occurs are inherently variable and dependent on the specific experimental setup and context.¹¹ As a result, the volumes and concentrations at phase equilibrium may exhibit significant variability. Fig. S1 in the ESI† compares the binodal curves obtained in this study with those previously reported in the literature. The observed differences are minimal, supporting the conclusion that the methodology employed is robust and reliable.

After constructing the binodal curves for the ATPS under investigation, it was necessary to define the boundaries of the two-phase region. This was achieved using the Merchuk equation (eqn (1)).^{22,24} The parameters A , B , and C , along with their respective standard deviations, are provided in Table S1 (ESI†). The results demonstrate a strong correlation between the experimental and calculated data.²⁵ Operating points were selected to ensure that the concentration of the phase-forming components in each ATPS yielded a phase volume ratio ($V_{\text{PP}}/V_{\text{SP}}$) of 1 (see Fig. 3). The conditions were defined such that the first operating point (FOP) was located near the binodal curve, while the last operating point (LOP) was positioned farther from it. Based on the theoretical tie-lines, the equilibrium concentrations of polymer and salt in both the polymer and saline phases were determined. These data are summarized in Table 4.

3.2. Sodium diclofenac extraction

The extraction of DFC was evaluated at an initial concentration of 10 ppm for both selected operating points. Table 4 presents the initial concentrations chosen for each operating point used in the DFC recovery experiments, along with the corresponding equilibrium concentrations derived from the theoretical tie-lines calculated for each condition.

Table 5 presents the results of the extraction process performed using a $[\text{DFC}] = 10$ ppm, along with the standard deviations obtained from three independent replicates. The ATPS composed of PEG-400/Sodium citrate, PEG-1000/Sodium citrate, and PEG-1000/Sodium sulfate exhibited extraction efficiencies exceeding 99.9%. In contrast, the PEG-400/Sodium sulfate system showed slightly lower extraction efficiencies—94.2% for the first operating point (FOP) and 97.7% for the last operating point (LOP).

This reduced performance may be attributed to two main factors. First, the lower molecular weight of PEG in the PEG-400/Sodium sulfate system results in a polymer phase with decreased hydrophobicity compared to that formed with PEG-1000 ($M_w = 1000 \text{ g mol}^{-1}$). Second, the lower concentration of Na_2SO_4 —relative to the PEG-400/Sodium citrate system—leads to a weaker *salting-out* effect, thereby reducing the partitioning of the drug into the polymer phase and slightly diminishing extraction efficiency.



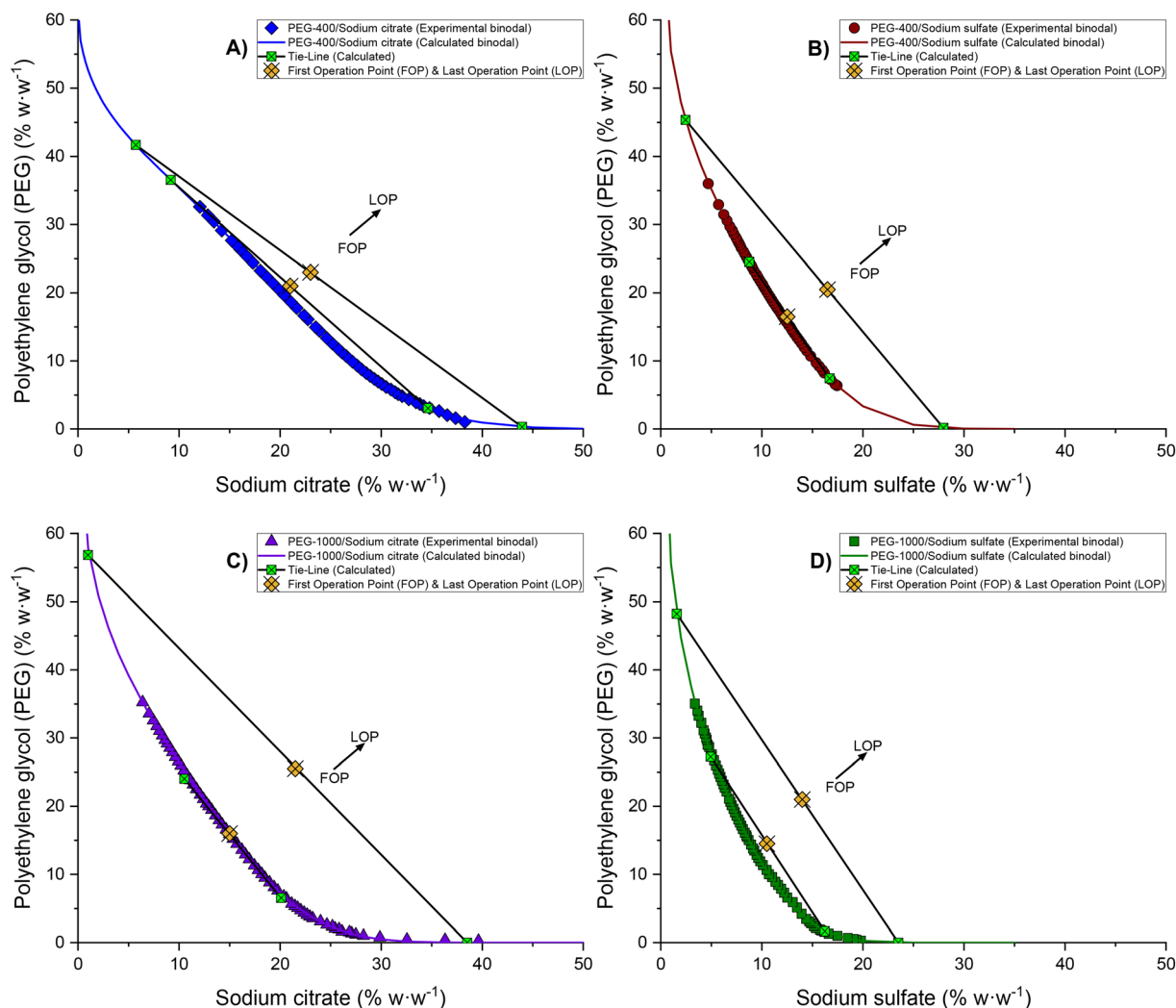


Fig. 3 Operating points ($V_{PP}/V_{SP} = 1$) used in the study of DFC recovery for each ATPS: PEG-400/Sodium citrate (◆), PEG-400/Sodium sulfate (●), PEG-1000/Sodium citrate (▲), PEG-1000/Sodium sulfate (■), at 298.15 K.

The DFC extraction results confirm that the process is highly efficient across all the ATPSs evaluated. Furthermore, an analysis of the total concentrations of the phase-forming components indicates that the concentrations of both PEG and salt are higher at the last operating point (LOP) compared to the first operating point (FOP). As a result, the presence of PEG in the saline phase (SP) and salt in the polymer phase (PP) at equilibrium is significantly reduced at the LOP relative to the FOP. This effect is further enhanced when using a higher molecular weight polymer (PEG-1000 g mol^{-1}).

These observations suggest that the LOP provides a more favorable environment for DFC extraction, and that PEG with a molecular weight of 1000 g mol^{-1} is the most suitable polymer for achieving maximum extraction efficiency.

3.3. Influence of phase volume ratio variation at the last operating point (LOP)

To assess the effect of phase volume ratio on the LOP, the same tie-line was employed while adjusting the initial concentrations of salt and polymer. This adjustment allowed for variation in

the phase volume ratio without altering the final equilibrium concentrations. Table 6 summarizes the initial concentrations of PEG and salt, the drug extraction percentage, the phase volume ratio, the concentration factor in the polymer phase, and the standard deviation for each experiment.

Notably, despite the changes in phase ratio, extraction efficiencies remained consistently above 99.9%, indicating the robustness of the system. In particular, for the ATPS composed of PEG-400/Sodium sulfate, an increase in drug extraction efficiency was observed, which can be attributed to the higher concentrations of both salt and polymer in the selected two-phase systems.

Overall, for the two-phase volume ratios evaluated in each ATPS, modifying the initial salt and polymer concentrations maintained high extraction efficiency. This finding is especially relevant from an industrial and environmental perspective, as it enables a reduction in reagent consumption, waste generation, and overall processing costs. Additionally, a notable concentration effect was observed, with DFC reaching up to 2.5 times its original concentration in the aqueous medium.



Table 4 Total concentrations of each ATPS under FOP and LOP conditions, for a volume ratio ($R = (V_{PP}/V_{SP}) = 1$), and their corresponding theoretical equilibrium concentrations of polymer and salt in the polymer phase and saline phase, at 298.15 K^a

	First operating point (FOP)					
	PEG-400/Sodium citrate			PEG-400/Sodium sulfate		
	Total system	PP	SP	Total system	PP	SP
Polymer (% w w ⁻¹)	21	36.55	3.05	16.5	24.53	7.44
Salt (% w w ⁻¹)	21	9.18	34.63	12.5	8.75	16.71
	PEG-1000/Sodium citrate					
	PEG-1000/Sodium citrate			PEG-1000/Sodium sulfate		
	Total system	PP	SP	Total system	PP	SP
Polymer (% w w ⁻¹)	16	24.03	6.53	14.5	27.24	1.66
Salt (% w w ⁻¹)	15	10.52	20.10	10.5	4.94	16.23
	Last operating point (LOP)					
	PEG-400/Sodium citrate			PEG-400/Sodium sulfate		
	Total system	PP	SP	Total system	PP	SP
Polymer (% w w ⁻¹)	23	41.69	0.31	20.5	45.37	0.15
Salt (% w w ⁻¹)	23	5.72	43.95	16.5	2.45	27.98
	PEG-1000/Sodium citrate					
	PEG-1000/Sodium citrate			PEG-1000/Sodium sulfate		
	Total system	PP	SP	Total system	PP	SP
Polymer (% w w ⁻¹)	25.5	56.83	0.0003	21	48.24	0.0002
Salt (% w w ⁻¹)	21.5	0.99	38.51	14	1.59	23.51

^a PP: polymer phase; SP: saline phase.

Table 5 Extraction percentage and standard deviation of DFC for each ATPS at 298.15 K^a

ATPS	Extraction (%)	Sd
PEG-400 g mol ⁻¹ /Sodium citrate	FOP	> 99.9
	LOP	0.2206
PEG-400 g mol ⁻¹ /Sodium sulfate	FOP	> 99.9
	LOP	0.3936
PEG-1000 g mol ⁻¹ /Sodium citrate	FOP	94.2
	LOP	0.7607
PEG-1000 g mol ⁻¹ /Sodium sulfate	FOP	97.7
	LOP	0.3740
PEG-400 g mol ⁻¹ /Sodium citrate	FOP	> 99.9
	LOP	0.9819
PEG-400 g mol ⁻¹ /Sodium sulfate	FOP	> 99.9
	LOP	1.2971
PEG-1000 g mol ⁻¹ /Sodium citrate	FOP	> 99.9
	LOP	1.9922
PEG-1000 g mol ⁻¹ /Sodium sulfate	FOP	> 99.9
	LOP	1.4663

^a Sd = standard deviation; FOP = first operating point; LOP = last operating point.

3.4. Influence of initial DFC concentration and pH on extraction efficiency

The extraction of DFC was evaluated as a function of its initial concentration (ranging from 10 to 1000 ppm) for each of the ATPS systems studied, considering the two operating points: the FOP and the LOP, with a phase volume ratio $R = (V_{PP}/V_{SP}) = 1$. For each condition, the pH of both phases was measured after the extraction process. The results are presented in Fig. 4 for

DFC extraction in citrate-based media, and in Fig. 5 for extraction in sulfate-based media.

As illustrated in Fig. 4A–D, the Na₃Cit-based systems exhibited high extraction efficiencies under both FOP and LOP conditions (extraction% >99.9%) across the entire range of initial DFC concentrations. Subsequent analyses will demonstrate the correlation between this behavior and the pH of the medium.

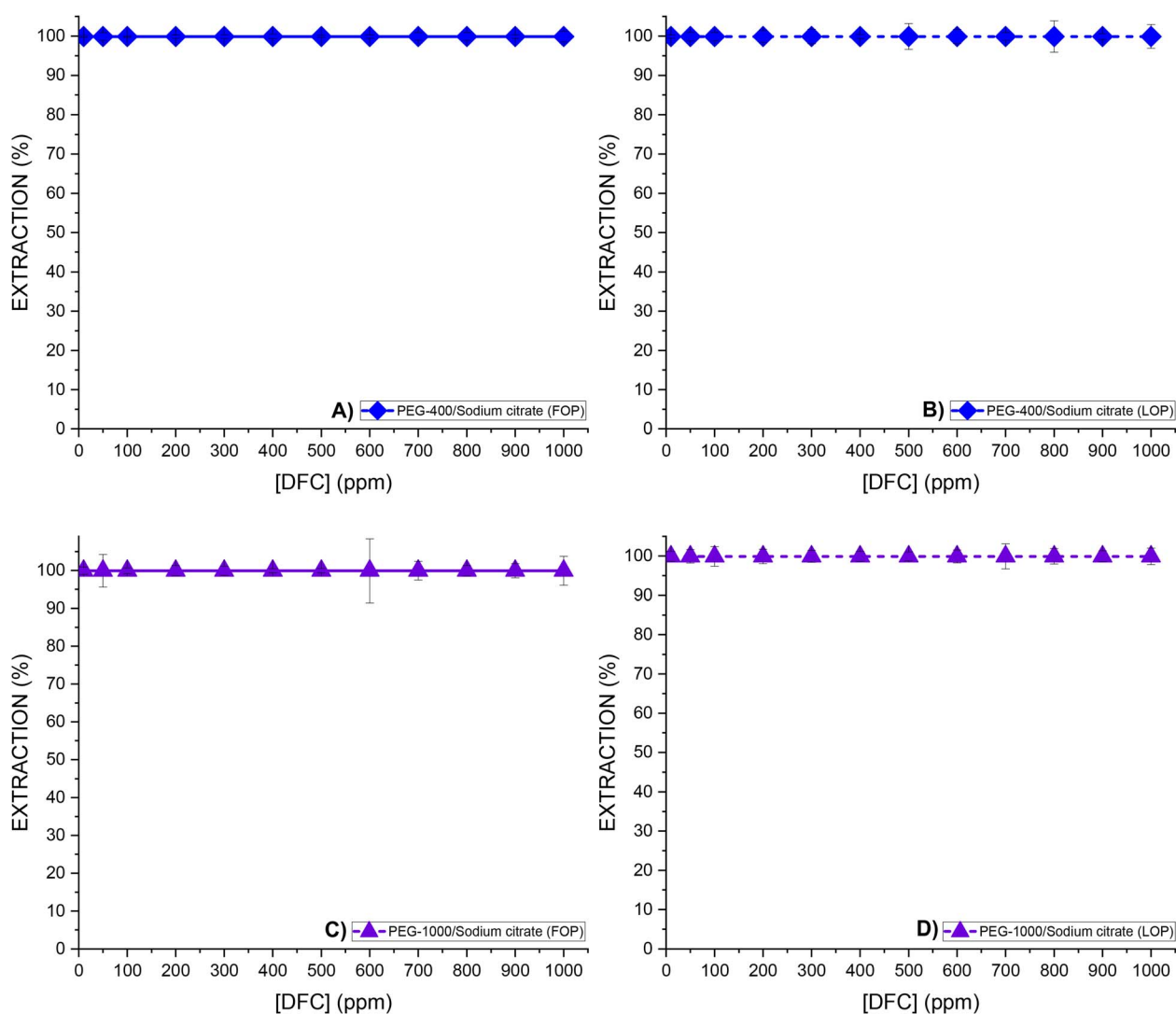
In contrast, the behavior of the systems with Na₂SO₄ is quite different (see Fig. 5). A consistent decrease in extraction efficiency ($R\%$) was observed as the concentration of the drug increased. Under FOP conditions (Fig. 5A and C), this reduction in $R\%$ occurred at relatively low DFC concentrations for both PEG-400 and PEG-1000. While, under LOP conditions (Fig. 5B and D), $R\%$ remained close to 99% at approximately 400 ppm and 700 ppm for PEG-400 and PEG-1000, respectively. Notably, in the sulfate-based medium, the decline in $R\%$ was accompanied by the formation of a DFC precipitate. Despite this precipitation occurring in the saline phase, the evaluation of extraction efficiency remains valid, as it is determined based on the composition of the polymer phase.

Accordingly, $R\%$ in the sulfate medium may decrease to values ranging from 75% to 20%, depending on the extent of precipitation. As will be further discussed, this behavior is



Table 6 Initial concentrations of PEG and salt, extraction percentages of diclofenac (at [DFC] = 10 ppm), phase volume ratio, concentration factor, and standard deviation for each ATPS under LOP conditions at 298.15 K^a

ATPS	Initial concentrations (% w·w ⁻¹)		Volume ratio	Concentration factor in PP	Extraction (%)	Sd
	PEG	Salt				
PEG-400 g mol ⁻¹ /Sodium citrate	30	17	1.9	0.52	>99.9	1.03
	15	30	0.4	2.5	>99.9	0.84
PEG-400 g mol ⁻¹ /Sodium sulfate	28	13	1.8	0.55	>99.9	0.62
	14	20	0.5	2.0	>99.9	2.94
PEG-1000 g mol ⁻¹ /Sodium citrate	36	15	2.2	0.45	>99.9	7.56
	16	28	0.5	2.0	>99.9	2.45
PEG-1000 g mol ⁻¹ /Sodium sulfate	30	10	2	0.5	>99.9	6.30
	12	18	0.5	2.0	>99.9	0.52

^a PP = polymer phase; SP = salt phase; Sd = standard deviation.**Fig. 4** Extraction percentages of DFC as a function of its initial concentration ([DFC]) in ATPS composed of: (A and B) PEG-400/Sodium citrate and (C and D) PEG-1000/Sodium citrate, under FOP and LOP conditions at 298.15 K.

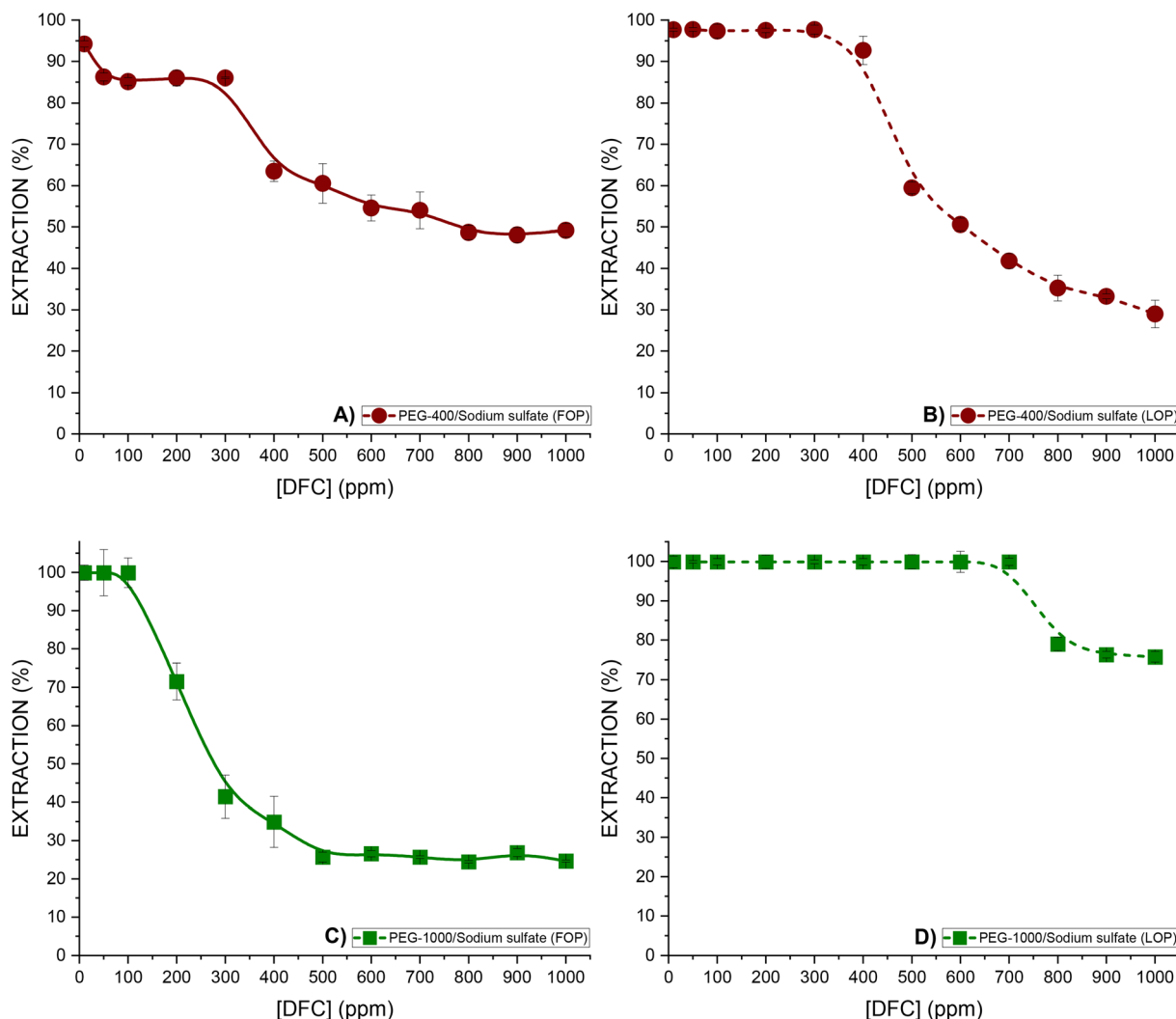


Fig. 5 Extraction percentages of DFC as a function of its initial concentration ([DFC]) in ATPS composed of: (A and B) PEG-400/Sodium sulfate and (C and D) PEG-1000/Sodium sulfate, under FOP and LOP conditions at 298.15 K.

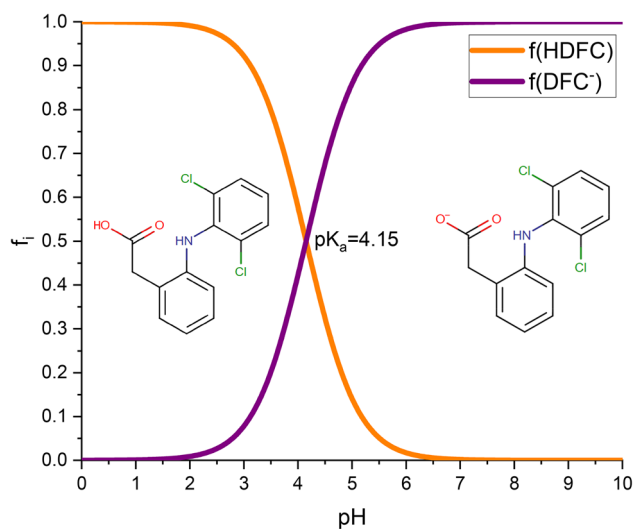


Fig. 6 Species distribution diagram of diclofenac as a function of pH.

closely related to the nature of the salt (*e.g.*, the pH of the medium), its concentration, and both the concentration and molecular weight of the PEG present in the polymer phase.

To understand the above results, it is necessary to identify the chemical species of DFC as a function of pH using a species distribution diagram.

The DFC species distribution diagram as a function of pH, shown in Fig. 6, was made considering the chemical equilibrium (represented by eqn (9) and eqn (10) and (11), where f_{DFC^-} and f_{HDFC} are the fractions of the protonated and deprotonated drug, respectively, as a function of the concentration of protons $[\text{H}^+]$ and the value of its acid dissociation constant ($K_a = \frac{1}{\beta_1}$).



$$f_{\text{DFC}^-} = \frac{1}{1 + \beta_1[\text{H}^+]} \quad (10)$$



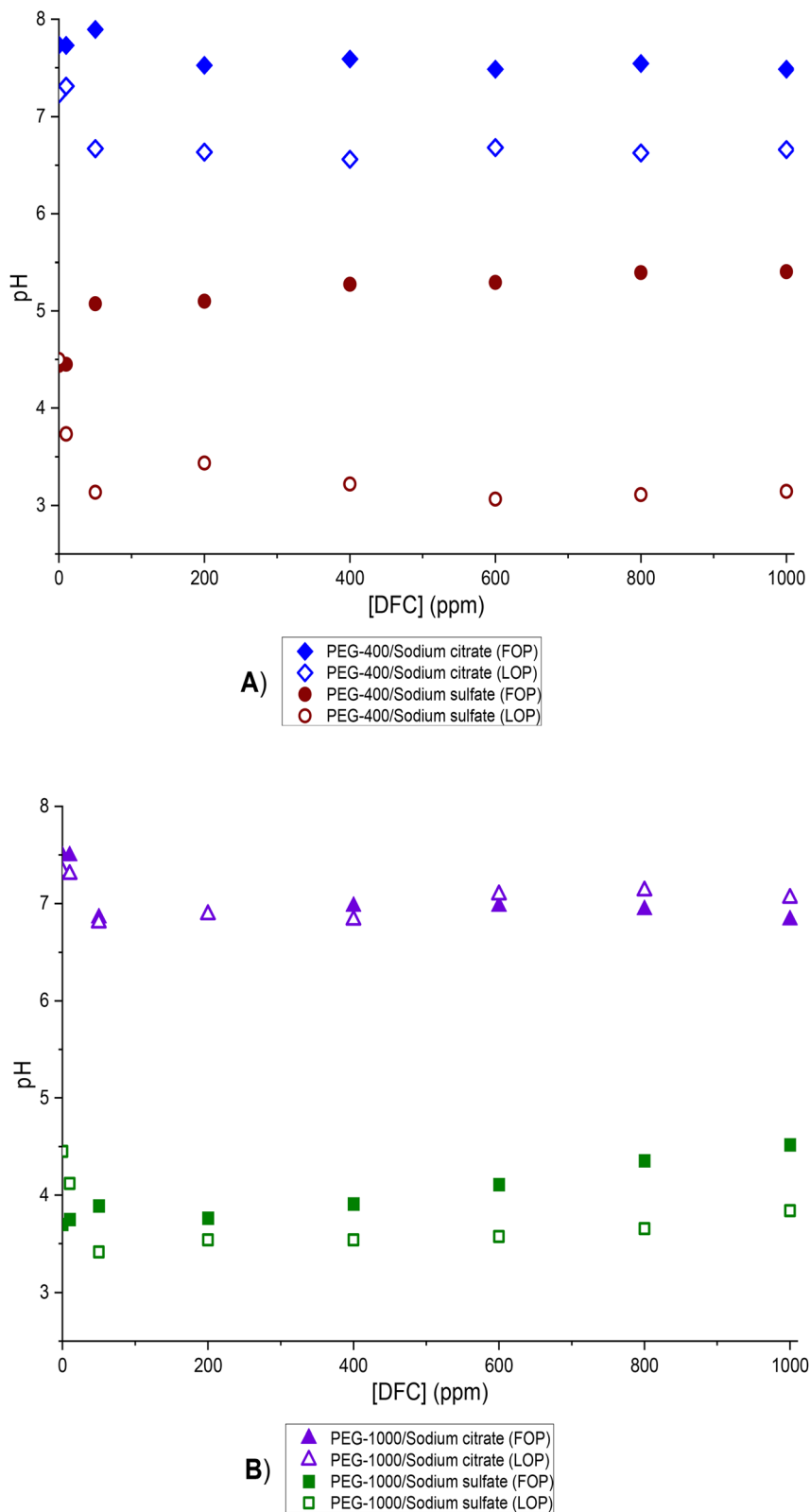


Fig. 7 pH variation as a function of DFC concentration for the different systems studied at 298.15 K. (A) ATPS composed of PEG-400/salt/H₂O; (B) ATPS composed of PEG-1000/salt/H₂O.

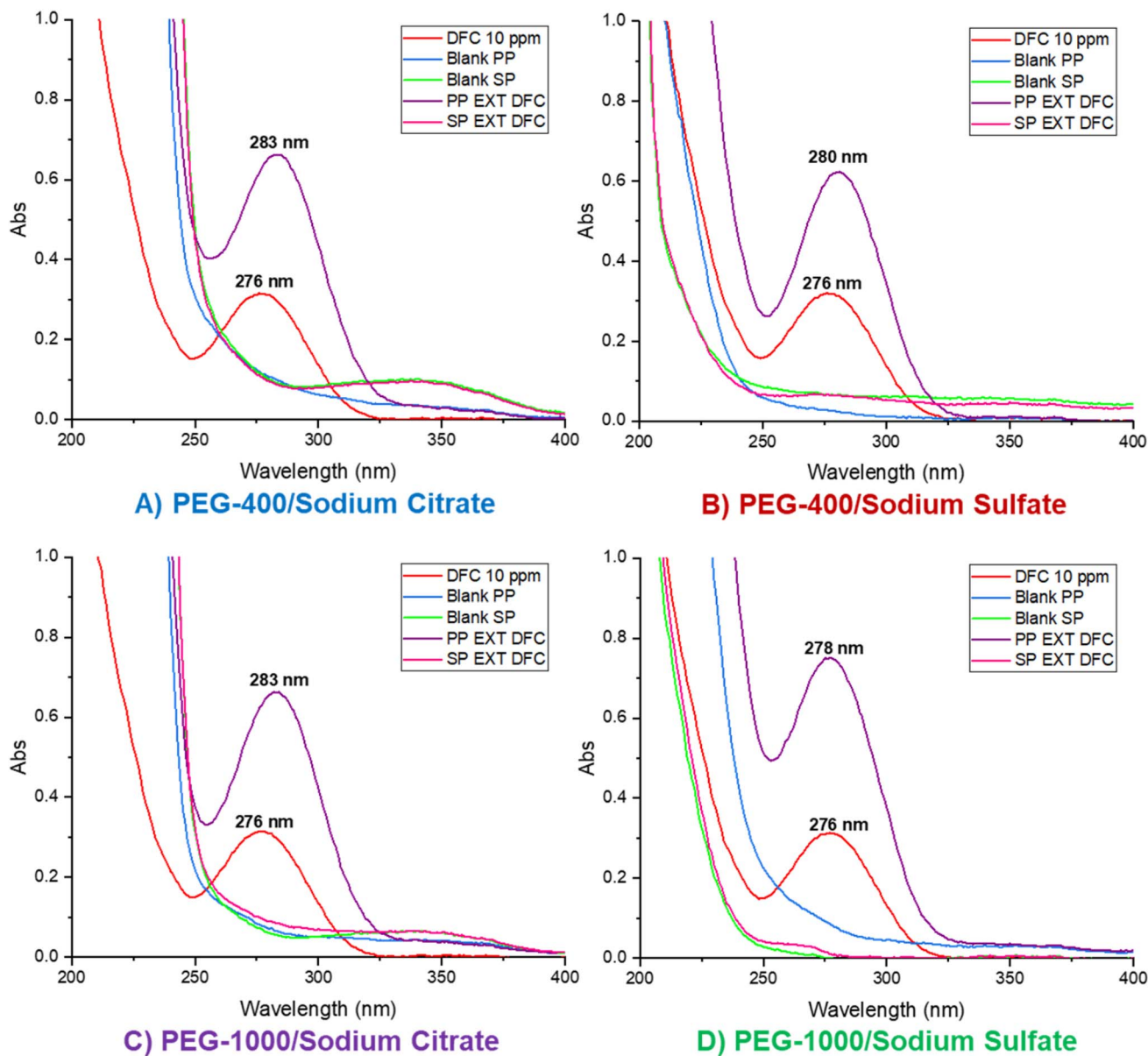


Fig. 8 UV-Vis spectral behavior during the DFC extraction process in ATPS under LOP conditions: (A) PEG-400/Sodium citrate, (B) PEG-400/Sodium sulfate, (C) PEG-1000/Sodium citrate, and (D) PEG-1000/Sodium sulfate.

$$f_{\text{HDFC}} = \frac{\beta_1[\text{H}^+]}{1 + \beta_1[\text{H}^+]} \quad (11)$$

Fig. 6 shows that the neutral form (HDFC) of diclofenac is the predominant species at pH values below 4.15 (pK_a value), while the DFC^- (deprotonated) species is the predominant species above this pH.

As previously mentioned, pH measurements were performed in both phases after DFC extraction for each of the systems studied. It was observed that the pH values in both phases were very similar; therefore, the pH values reported in Fig. 7(A and B) represent the average pH of both phases under each condition.

In the case of the Na_3Cit medium (FOP and LOP), the equilibrium pH is consistently above 6 (see Fig. 7A), which exceeds

the pK_a of DFC (4.15). Therefore, the predominant species in all cases is the deprotonated form, DFC^- , as shown in Fig. 6. As will be discussed later, this form of DFC is favorable for achieving high extraction efficiencies ($R\%$).

In contrast, in the sulfate-based medium, the minimum pH value is close to 3, and the highest is around pH 5.5 (see Fig. 7B). This implies that the protonated species, HDFC, may predominate at pH values below 4.15 (the pK_a of DFC), whereas the deprotonated form, DFC^- , becomes dominant above this threshold, as illustrated in Fig. 6.

The presence of the HDFC species significantly limits its solubility in the saline (sulfate) phase and competes with its solubility (or partitioning) in the polymer phase. This clearly explains the trends observed in Fig. 5A to D.



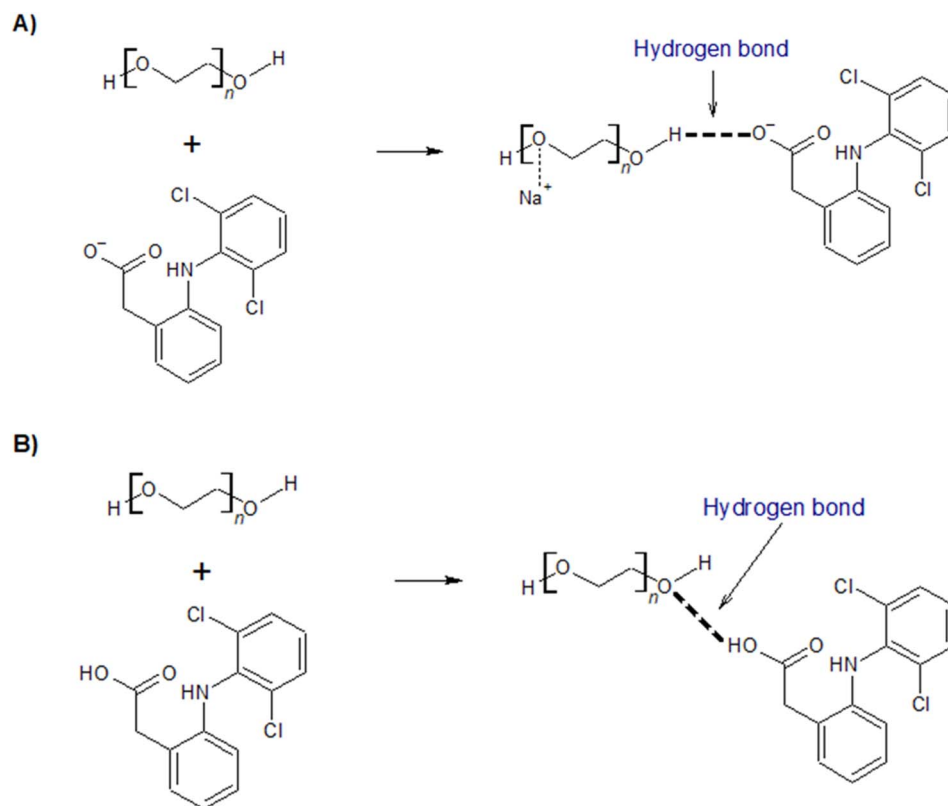


Fig. 9 Proposed mechanisms for drug extraction via hydrogen bonding between: (A) the terminal hydrogen of PEG and sodium diclofenac, and (B) the terminal oxygen of PEG and sodium diclofenac.

In conclusion, pH is a critical factor in the recovery process of DFC, as is the nature (pH controllability) and concentration (which influences the “salting out” effect) of each salt, as well as the concentration and molecular weight of the polymer. In all the systems studied, at low drug concentrations (10 ppm), high extraction efficiency was observed, suggesting that pH does not have a significant influence under these conditions. However, at concentrations higher than 10 ppm, pH becomes a relevant parameter, especially in the ATPS formed with sodium sulfate.

3.5. Analysis of the mass transfer process of DFC into the polymer phase

The mass transfer of DFC was investigated by analyzing the extraction process using UV-Vis absorption spectroscopy. Measurements were carried out for both phases of each ATPS at the LOP with an initial DFC concentration of 10 ppm. The corresponding spectra for the extracted DFC in each phase (PP EXT DFC and SP EXT DFC) were obtained. For comparison, the absorption spectra of DFC in aqueous solution (10 ppm), as well as the polymer and saline phases in the absence of DFC (blank PP and blank SP), are included in Fig. 8.

The drug in aqueous solution exhibits a maximum absorption peak at 276 nm, which is characteristic of DFC in this medium. In contrast, during the extraction process, when DFC is transferred to the polymer phase, an increase in

absorbance is observed—attributable to the concentration effect of DFC in the polymeric environment. Additionally, the DFC absorption profile in the polymer phase displays a distinct positive band shape compared to its spectrum in aqueous solution.

A bathochromic shift is also evident, with the absorption maximum shifting to wavelengths between 280 and 283 nm, depending on the specific ATPS. This enhanced signal and red shift are likely due to hydrogen bonding interactions between DFC and PEG.^{26–28} Notably, PEG is capable of forming a broad range of molecular associations due to its terminal primary hydroxyl groups, which can readily interact with various compounds and functional groups—including ethers, amines, fatty acids, and propylene glycols—among others.²⁹ These interactions suggest that complex formation between DFC and PEG is a plausible mechanism contributing to the observed spectral behavior.

In light of the observations above and the changes in behavior observed during the DFC extraction process as a function of pH, we propose two possible mechanisms for drug extraction.

In the first mechanism (Fig. 9A), at pH values above the pK_a of DFC (Fig. 6), the drug exists predominantly in its anionic form (DFC⁻). In this state, the hydroxyl hydrogen atoms of the PEG chain may form hydrogen bonds with the negatively charged oxygen atom of the carboxyl group in DFC⁻. Additionally, the sodium counterion (Na⁺) may associate with the



ether oxygen atoms of the PEG chain, contributing to charge neutralization within the polymer phase.

In the second mechanism (Fig. 9B), at pH values below the pK_a , DFC is present primarily in its neutral (acidic) form (HDFC). Under these conditions, hydrogen bonding may occur between the ether oxygen atoms of PEG and the hydrogen atom of the carboxylic group in HDFC.

In both mechanisms, the formation of hydrogen bonds induces an electron redistribution within the DFC molecule. This redistribution lowers the molecular energy and leads to a red shift in the absorption maximum (*i.e.*, an increase in wavelength), as observed in Fig. 8 and consistent with previous findings.^{27,28} Given the structural characteristics of DFC, it is postulated that the phenylacetic acid moiety plays a central role in conferring the chromophoric properties of the molecule. This group contains a carbonyl functional group with non-bonding electron pairs on the oxygen atom, making it highly susceptible to electronic delocalization. Consequently, changes in electron distribution within this group are responsible for the observed shifts in the absorption wavelength.

Our findings are in good agreement with the studies conducted by Li *et al.*,^{27,28} who investigated the formation of hydrogen bonds between polyethylene glycol and various drugs in two independent works. In the first,²⁷ they analyzed a liquid–liquid extraction system composed of a non-ionic surfactant (PEG-1000), ammonium sulfate ((NH₄)₂SO₄), and water, applied to the extraction of chlorpromazine (CPZ) and procaine (PCN). The results showed a red shift in the UV-Vis absorption spectra upon transfer of the drugs to the PEG phase (254 → 256 nm for CPZ and 290 → 295 nm for PCN), indicating the formation of hydrogen bonds between PEG and the drugs, particularly in the case of PCN.

In a second study,²⁸ the authors extended the analysis to the distribution behavior of three drugs—CPZ, PCN, and procaine amide (PCNA)—in aqueous two-phase systems (ATPS) formed by PEG-800 or PEG-1500 and (NH₄)₂SO₄. Again, UV-Vis spectra revealed red shifts upon partitioning of the compounds into the PEG phase: +2 nm for CPZ, +3 nm for PCN, and +5 nm for PCNA. These findings further support the presence of hydrogen bonding interactions, which are more pronounced in PCNA due to its greater ability to form such bonds.

Therefore, this type of bathochromic shift caused by PEG–drug interactions within PEG/salt/water-based ATPS has been previously reported, thus supporting the findings observed in this study.

4 Conclusions

The results obtained in this study demonstrate that the extraction of sodium diclofenac using ATPS is highly efficient under most of the evaluated conditions, achieving extraction percentages greater than 99.9%, particularly in systems composed of PEG-1000 g mol⁻¹ to 25.5% w w⁻¹ and Na₃Cit to 21.5% w w⁻¹. It was identified that pH, the nature of salt, the concentration and molecular weight of the polymer, and the modification of the drug concentration are key factors in the

efficiency of the process. Furthermore, UV-Vis spectroscopic analysis suggests that the transfer of the drug to the polymer phase occurs through the formation of hydrogen bonds with PEG, contributing to the understanding of the partitioning mechanism.

From a sustainability perspective, the use of biodegradable and low-toxicity compounds such as PEG and sodium citrate, along with the predominantly aqueous nature of the system, positions ATPS as a green and viable alternative for environmental remediation.

However, although the scalability potential of the system is mentioned, this claim requires further evaluation. Industrial-scale implementation faces technical and economic challenges, such as the design of continuous processes, recovery and reuse of components, and integration with existing water treatment technologies. Economic feasibility will also depend on the cost of materials, the efficiency of the process at scale, and the regeneration of components without significant loss of performance.

Looking ahead, future research could focus on evaluating the scalability of the process through pilot studies that consider process engineering aspects, energy efficiency, and life cycle analysis; exploring the efficacy of the ATPS system in extracting other pharmaceutical contaminants such as antibiotics, hormones, and metabolites; optimizing the system formulation to maximize recovery with minimal input consumption, thereby reducing operational costs and environmental impact; investigating phase reuse and recovery of the extracted drug, which are essential for the sustainability of the process.

Overall, this work not only demonstrates the efficacy of the ATPS system for diclofenac recovery but also lays the groundwork for its development as a clean, efficient, and adaptable separation technology for various industrial and environmental applications.

Abbreviations

DFC	Diclofenac
ATPS	Aqueous two-phase systems
PEG	Polyethylene glycol
UV-Vis	Ultraviolet-visible
NSAID	Nonsteroidal anti-inflammatory drug
PP	Polymer phase
SP	Saline phase
FOP	First operation point
LOP	Last operation point
Sd	Standard deviation
wt ^{salt}	Percentage by weight of the salt
wt ^{PEG}	Percentage by weight of the polymer
wt ^{PEG} _{cal}	Percentage by weight of the polymer calculated
wt ^{PEG} _{exp}	Percentage by weight of the polymer experimental
<i>N</i>	Amount of data of the binodal curve
<i>U</i>	Minimization function
<i>R</i>	Volume ratio
<i>f_i</i>	Fraction of species <i>i</i>



Data availability

The data of submitted manuscript “Study Of Diclofenac Distribution In Aqueous Two-Phase Peg/Salt/Water Systems”, authored by Diana Esmeralda Martínez-Rodríguez, Edgar Daniel Martínez-Rodríguez, Liliana Hernández-Perales, María del Pilar González-Muñoz & Mario Avila-Rodríguez, could be found in the next link: <https://drive.google.com/drive/folders/1UDgANmLxZMQImtC1cn0HxOym3juzDT7Y?usp=sharing>.

Author contributions

Diana Esmeralda Martínez-Rodríguez: conceptualization, methodology, investigation, formal analysis, writing – original draft, writing – review & editing, Visualization. Edgar Daniel Martínez-Rodríguez: methodology, software, investigation, writing – review & editing. Liliana Hernández-Perales: supervision, writing – review & editing. María del Pilar González-Muñoz: supervision, writing – review & editing. Mario Avila-Rodríguez: conceptualization, methodology, investigation, resources, writing – review & editing, visualization, supervision, funding acquisition.

Conflicts of interest

There are no conflicts of interest to declare.

Acknowledgements

The authors would like to thank LANCAPFEM UG-UAA for the analysis services, “POLIOLES S.A. de C.V” for providing PEG, SECIHTI (CB 259307 project), and the ‘Universidad de Guanajuato’ (55-2024 project) for the financial support. Diana Esmeralda Martínez-Rodríguez thanks the Universidad de Guanajuato and SECIHTI (grant 926294).

References

- M. Gil, A. Soto, J. Usma and O. Gutiérrez, Contaminantes emergentes en aguas, efectos y posibles tratamientos, *Producción más limpia*, 2012, 7, 52–73, DOI: [10.22507/pml](https://doi.org/10.22507/pml).
- Y. Zhang, S. Geißen and C. Gal, Carbamazepine and diclofenac: Removal in wastewater treatment plants and occurrence in water bodies, *Chemosphere*, 2008, 73, 1151–1161, DOI: [10.1016/j.chemosphere.2008.07.086](https://doi.org/10.1016/j.chemosphere.2008.07.086).
- PubChem, Diclofenac, Bethesda (MD): National Center for Biotechnology Information, 2020, available from: <https://pubchem.ncbi.nlm.nih.gov/compound/diclofenac#section=Chemical-and-Physical-Properties>.
- US National Library of Medicine, Diclofenac, Bethesda (MD), MedlinePlus, 2020, available from: <https://medlineplus.gov/spanish/druginfo/meds/a689002-es.html>.
- A. Abadi, A. Eissa and G. Hassan, Synthesis of novel 1,3,4-trisubstituted pyrazole derivatives and their evaluation as antitumor and antiangiogenic agents, *Chem. Pharm. Bull.*, 2003, 51, 838–844, DOI: [10.1248/cpb.51.838](https://doi.org/10.1248/cpb.51.838).
- M. Gómez-Lechón, X. Ponsoda, E. O'Connor, T. Donato, R. Jover and J. Castell, Diclofenac induces apoptosis in hepatocytes, *Toxicol. In Vitro*, 2003, 17, 675–680, DOI: [10.1016/S0887-2333\(03\)00105-X](https://doi.org/10.1016/S0887-2333(03)00105-X).
- P. Sathishkumar, R. A. Meena, T. Palanisami, V. Ashokkumar, T. Palvannan and F. L. Gu, Occurrence, interactive effects and ecological risk of Diclofenac in environmental compartments and biota— a review, *Sci. Total Environ.*, 2020, 698, 134057, DOI: [10.1016/j.scitotenv.2019.134057](https://doi.org/10.1016/j.scitotenv.2019.134057).
- J. Schwaiger, H. Ferling, U. Mallow, H. Wintermayr and R. Negele, Toxic effects of the nonsteroidal anti-inflammatory drug diclofenac: Part I: histopathological alterations and bioaccumulation in rainbow trout, *Aquat. Toxicol.*, 2004, 68, 141–150, DOI: [10.1016/j.aquatox.2004.03.014](https://doi.org/10.1016/j.aquatox.2004.03.014).
- S. C. Silvério, A. Wegrzyn, E. Lladosa, O. Rodríguez and E. A. Macedo, Effect of aqueous two-phase system constituents in different poly(ethylene glycol)–salt phase diagrams, *J. Chem. Eng. Data*, 2012, 57, 1203–1208, DOI: [10.1021/je2012549](https://doi.org/10.1021/je2012549).
- M. Iqbal, Y. Tao, S. Xie, Y. Zhu, D. Chen, X. Wang, *et al.*, Aqueous two-phase system (ATPS): an overview and advances in its applications, *Biol. Proced. Online*, 2016, 18, 18, DOI: [10.1186/s12575-016-0048-8](https://doi.org/10.1186/s12575-016-0048-8).
- Aqueous Two-phase Systems: Methods and Protocols*, ed. R. Hatti-Kaul, Springer, New York, 2000, vol. 11, DOI: [10.1385/1592590284](https://doi.org/10.1385/1592590284).
- C. X. Li, J. Han, Y. Wang, Y. S. Yan, X. H. Xu and J. M. Pan, Extraction and mechanism investigation of trace roxithromycin in real water samples by use of ionic liquid–salt aqueous two-phase system, *Anal. Chim. Acta*, 2009, 653, 178–183, DOI: [10.1016/j.aca.2009.09.011](https://doi.org/10.1016/j.aca.2009.09.011).
- M. Shao, X. Zhang, N. Li, J. Shi, H. Zhang, Z. Wang, *et al.*, Ionic liquid-based aqueous two-phase system extraction of sulfonamides in milk, *J. Chromatogr. B*, 2014, 961, 5–12, DOI: [10.1016/j.jchromb.2014.04.054](https://doi.org/10.1016/j.jchromb.2014.04.054).
- J. F. Pereira, F. Vicente, V. C. Santos-Ebinuma, J. M. Araújo, A. Pessoa, M. G. Freire, *et al.*, Extraction of tetracycline from fermentation broth using aqueous two-phase systems composed of polyethylene glycol and cholinium-based salts, *Process Biochem.*, 2013, 48, 716–722, DOI: [10.1016/j.procbio.2013.02.025](https://doi.org/10.1016/j.procbio.2013.02.025).
- P. A. J. Rosa, I. F. Ferreira, A. M. Azevedo and M. R. Aires-Barros, Aqueous two-phase systems: a viable platform in the manufacturing of biopharmaceuticals, *J. Chromatogr. A*, 2010, 1217, 2296–2305, DOI: [10.1016/j.chroma.2009.11.034](https://doi.org/10.1016/j.chroma.2009.11.034).
- R. C. Assis, A. B. Mageste, L. R. de Lemos, R. M. Orlando and G. D. Rodrigues, Application of aqueous two-phase systems for the extraction of pharmaceutical compounds from water samples, *J. Mol. Liq.*, 2020, 301, 112411, DOI: [10.1016/j.molliq.2019.112411](https://doi.org/10.1016/j.molliq.2019.112411).
- J. A. Asenjo and B. A. Andrews, Aqueous two-phase systems for protein separation: a perspective, *J. Chromatogr. A*, 2011, 1218, 8826–8835, DOI: [10.1016/j.chroma.2011.06.051](https://doi.org/10.1016/j.chroma.2011.06.051).
- Q. Liu, J. Yu, W. Li, X. Hu, H. Xia, H. Liu, *et al.*, Partitioning behavior of penicillin G in aqueous two phase system



- formed by ionic liquids and phosphate, *Sep. Sci. Technol.*, 2006, **41**, 2849–2858, DOI: [10.1080/01496390600786135](https://doi.org/10.1080/01496390600786135).
- 19 M. González-González, M. Rito-Palomares and O. Méndez-Quintero, Partition behavior of CD133+ stem cells from human umbilical cord blood in aqueous two-phase systems: in route to establish novel stem cell primary recovery strategies, *Biotechnol. Prog.*, 2014, **30**, 700–707, DOI: [10.1002/btpr.1875](https://doi.org/10.1002/btpr.1875).
- 20 M. Baghbanbashi, H. S. Shiran, A. Kakkar, G. Pazuki and K. Ristroph, Recent advances in drug delivery applications of aqueous two-phase systems, *PNAS Nexus*, 2024, **3**, 255, DOI: [10.1093/pnasnexus/pgae255](https://doi.org/10.1093/pnasnexus/pgae255).
- 21 F. Luechau, T. C. Ling and A. Lyddiatt, Partition of plasmid DNA in polymer–salt aqueous two-phase systems, *Sep. Purif. Technol.*, 2009, **66**, 397–404, DOI: [10.1016/j.seppur.2008.12.003](https://doi.org/10.1016/j.seppur.2008.12.003).
- 22 F. G. Ahsaie, G. Pazuki, T. E. Sintra, P. Carvalho and S. P. Ventura, Study of the partition of sodium diclofenac and norfloxacin in aqueous two-phase systems based on copolymers and dextran, *Fluid Phase Equilib.*, 2021, **530**, 112868, DOI: [10.1016/j.fluid.2020.112868](https://doi.org/10.1016/j.fluid.2020.112868).
- 23 V. P. Priyanka and R. L. Gardas, Mono- and di-cationic ionic liquids based aqueous biphasic systems for the extraction of diclofenac sodium, *Sep. Purif. Technol.*, 2020, **234**, 116048, DOI: [10.1016/j.seppur.2019.116048](https://doi.org/10.1016/j.seppur.2019.116048).
- 24 J. C. Merchuk, B. A. Andrews and J. A. Asenjo, Aqueous two-phase systems for protein separation: studies on phase inversion, *J. Chromatogr. B: Biomed. Sci. Appl.*, 1998, **711**, 285–293, DOI: [10.1016/S0378-4347\(97\)00594-X](https://doi.org/10.1016/S0378-4347(97)00594-X).
- 25 M. T. Zafarani-Moattar and S. Tolouei, Liquid-liquid equilibria of aqueous two-phase systems containing polyethylene glycol 4000 and di-potassium tartrate, potassium sodium tartrate, or di-potassium oxalate: Experiment and correlation, *Calphad*, 2008, **32**, 655–660, DOI: [10.1016/j.calphad.2008.09.006](https://doi.org/10.1016/j.calphad.2008.09.006).
- 26 A. S. Murthy and C. N. R. Rao, Spectroscopic studies of the hydrogen bond, *Appl. Spectrosc. Rev.*, 1968, **2**, 69–191, DOI: [10.1080/05704926808050887](https://doi.org/10.1080/05704926808050887).
- 27 L. Li, F. Liu, X. Kong, S. Su and K. A. Li, Investigation of a liquid-liquid extraction system based on non-ionic surfactant–salt–H₂O and mechanism of drug extraction, *Anal. Chim. Acta*, 2002, **452**, 321–328, DOI: [10.1016/S0003-2670\(01\)01471-4](https://doi.org/10.1016/S0003-2670(01)01471-4).
- 28 L. Li, C. Y. He, S. H. Li, F. Liu, S. Su, X. X. Kong, *et al.*, Study on PEG-(NH₄)₂SO₄ aqueous two-phase system and distribution behavior of drugs, *Chin. J. Chem.*, 2004, **22**, 1313–1318, DOI: [10.1002/cjoc.20040221120](https://doi.org/10.1002/cjoc.20040221120).
- 29 H. Jang, C. Shin and K. Kim, Safety evaluation of polyethylene glycol (PEG) compounds for cosmetic use, *Toxicol. Res.*, 2015, **31**, 105–136, DOI: [10.5487/TR.2015.31.2.105](https://doi.org/10.5487/TR.2015.31.2.105).

